Neuropsychopharmacology (2011) 36, 1871–1878

www.neuropsychopharmacology.org

The *ZNF804A* Gene: Characterization of a Novel Neural Risk Mechanism for the Major Psychoses

Aristotle N Voineskos*[,1], Jason P Lerch[2,3], Daniel Felsky[1], Arun Tiwari[1], Tarek K Rajji[1], Dielle Miranda[1], Nancy J Lobaugh[4], Bruce G Pollock[1], Benoit H Mulsant[1] and James L Kennedy[1]

[1]Department of Psychiatry, Centre for Addiction and Mental Health, University of Toronto, Toronto, Canada; [2]Department of Medical Biophysics, Toronto Centre for Phenogenomics and Hospital for Sick Children, University of Toronto, Toronto, Canada; [3]Neurosciences and Mental Health, Hospital for Sick Children, University of Toronto, Toronto, Canada; [4]Cognitive Neurology, Sunnybrook Health Sciences Centre, Department of Medicine, University of Toronto, Toronto, Canada

Schizophrenia and bipolar disorder share genetic risk, brain vulnerability, and clinical symptoms. The *ZNF804A* risk variant, rs1344706, confers susceptibility for both disorders. This study aimed to identify neural mechanisms common to both schizophrenia and bipolar disorder through this variant's potential effects on cortical thickness, white matter tract integrity, and cognitive function. Imaging, genetics, and cognitive measures were ascertained in 62 healthy adults aged between 18 and 59 years. High-resolution multimodal MRI/DTI imaging was used to measure cortical thickness and major frontotemporal and interhemispheric white matter tracts. The general linear model was used to examine the influence of the *ZNF804A* rs1344706 risk variant on cortical thickness, white matter tract integrity, and cognitive measures. Individuals homozygous for the risk variant ('A' allele) demonstrated reduced cortical gray matter thickness in the superior temporal gyrus, and in the anterior and posterior cingulate cortices compared with C-allele carriers. No effect of the risk variant on microstructural integrity of white matter tracts was found. Reduced attention control was found in risk allele homozygotes, aligning with findings in the anterior cingulate cortex. Our data provide a novel, genetically based neural risk mechanism for the major psychoses by effects of the *ZNF804A* risk variant on neural structures and cognitive function susceptible in both disorders. Our findings link genetic, imaging, and cognitive susceptibility relevant to both schizophrenia and bipolar disorder.
Neuropsychopharmacology (2011) **36,** 1871–1878; doi:10.1038/npp.2011.72; published online 27 April 2011

Keywords: *ZNF804A*; cortical thickness; DTI; white matter; schizophrenia; bipolar disorder

INTRODUCTION

Although unique genetic factors are likely involved, there is now compelling evidence from population genetic (Lichtenstein *et al*, 2009) and genome-wide association (Purcell *et al*, 2009; Williams *et al*, 2011) studies that suggests that schizophrenia and bipolar disorder share considerable genetic risk. One of the most strongly associated (and replicated) genome-wide significant risk variant conferring risk for both schizophrenia and bipolar disorder is the rs1344706 single-nucleotide polymorphism (SNP), located within the zinc-finger protein 804A (*ZNF804A*) gene (O'Donovan *et al*, 2008; Purcell *et al*, 2009). *In silico* work predicts that this variant may act as a binding site for a myelin transcription factor, serving as a link to shared findings of oligodendrocyte and myelin disruption in the postmortem brain in both schizophrenia and bipolar disorder (Riley *et al*, 2010). *In vivo*, evidence has accumulated that corticocortical white matter tracts may be disrupted in schizophrenia (Voineskos *et al*, 2010b) and in bipolar disorder (McIntosh *et al*, 2008). However, postmortem data demonstrating oligodendrocyte gene downregulation and reduced oligodendrocyte number in these disorders emerge primarily from studies that have sampled tissues from the cortical gray matter (Tkachev *et al*, 2003). Therefore, we hypothesized that the *ZNF804A* variant may exert its effects on the cortical gray matter, white matter tracts connecting cortical gray matter regions, or both, to confer risk for schizophrenia and bipolar disorder.

Although there have been recent examinations of the *ZNF804A* variant in conjunction with structural (volumetric) MRI approaches (Donohoe *et al*, 2011; Lencz *et al*, 2010), no investigation, to our knowledge, has yet examined the effects of *ZNF804A* (or any other genome-wide significant risk variants) on more refined MRI phenotypes of cortical thickness or white matter tract integrity. These

*Correspondence: Dr AN Voineskos, Centre for Addiction and Mental Health, 250 College Street, Toronto, ON, Canada, M5T 1R8, Tel: +1 416 535 8501 4378, Fax: +1 416 979 6936,
E-mail: Aristotle_Voineskos@camh.net
Received 31 January 2011; revised 6 March 2011; accepted 28 March 2011

MRI-based phenotypes can provide unique information regarding cortical gray matter and white matter. Cortical thickness mapping tools can be used to pinpoint differences in cortical thickness at submillimetric resolution between study populations (Lerch and Evans, 2005). This allows for considerable refinement of earlier volumetric approaches. Cortical thickness measurements are meaningful quantitatively and are operator independent. Similarly, diffusion tensor imaging is a considerable improvement over volumetric MRI studies of the white matter, as DTI can be used to measure the white matter in a manner not possible with conventional MRI (Alexander and Lobaugh, 2007). In particular, DTI tractography can be used to measure major white matter connections between brain regions that are essential for effective corticocortical communication (Catani *et al*, 2002). Although there are unique findings for each disorder, recent evidence is emerging suggesting that alterations in cortical thickness (Rimol *et al*, 2010) and white matter tract integrity (McIntosh *et al*, 2008) may be shared neural vulnerability phenotypes for schizophrenia and bipolar disorder.

In MRI studies of schizophrenia, a characteristic cortical gray matter finding has been superior temporal gyrus volume reduction, and this structure even experiences reduction during transition to psychosis (Takahashi *et al*, 2009). However, this region is often affected in bipolar disorder as well. Conversely, reduction in the volume of the anterior cingulate cortex is arguably the most well-established gray matter finding in bipolar disorder (Bora *et al*, 2010), although this region is also affected in schizophrenia (Fornito *et al*, 2009; Narr *et al*, 2005). Using DTI, key frontotemporal and interhemispheric white matter tracts have been implicated in both schizophrenia (Voineskos *et al*, 2010b; Whitford *et al*, 2010) and bipolar disorder (McIntosh *et al*, 2008). DTI tractography provides the opportunity to test whether the *ZNF804A* variant's recently demonstrated effects on frontotemporal and prefrontal interhemispheric functional disconnectivity are mediated by white matter tracts connecting those regions (Esslinger *et al*, 2009). Finally, in terms of cognitive function, attention control is considered a primary overlapping deficit between schizophrenia and bipolar disorder, although working memory and verbal episodic memory performance are also affected in both disorders (Hill *et al*, 2008). Therefore, we proceeded to examine whether the *ZNF804A* risk variant influences cortical thickness, white matter tract integrity, and cognitive performance to confer an intermediate risk phenotype for the major psychoses.

MATERIALS AND METHODS

Participants

A total of 62 healthy Caucasian volunteers met the inclusion criteria (age between 18 and 59 years; right handedness) and none of the exclusion criteria (any history of a mental disorder, current substance abuse, or a history of substance dependence; positive urine toxicology, a history of head trauma with loss of consciousness, seizure, or another neurological disorder; a first-degree relative with a history of psychotic mental disorder). All participants were assessed using the Edinburgh handedness inventory (Oldfield, 1971), the Wechsler Test for Adult Reading, and the Hollingshead index (Hollingshead, 1975); all were interviewed by a psychiatrist, and completed the Structured Clinical Interview for DSM-IV Disorders (First *et al*, 1995). They also completed a urine toxicology screen. The study was approved by the Research Ethics Board of the Centre for Addiction and Mental Health (Toronto, Canada), and all participants provided informed, written consent.

Neuroimaging

Image acquisition. High-resolution magnetic resonance images were acquired as part of a multi-modal imaging protocol using an eight-channel head coil on a 1.5-T GE Echospeed system (General Electric Medical Systems, Milwaukee, WI), which permits maximum gradient amplitudes of 40 mT/m. Axial inversion recovery-prepared spoiled gradient recall images were acquired: (echo time (TE): 5.3, repetition time (TR): 12.3, time to inversion: 300, flip angle 20, number of excitations = 1 (124 contiguous images, 1.5 mm thickness). For DTI acquisition, a single-shot spin-echo planar sequence was used with diffusion gradients applied in 23 non-collinear directions and $b = 1000$ s/mm^2. Two $b = 0$ images were obtained. A total of 57 slices were acquired for whole-brain coverage oblique to the axial plane. Slice thickness was 2.6 mm, and voxels were isotropic. The field of view was 330 mm, and the size of the acquisition matrix was 128×128 mm^2, with TE = 85.5 ms and TR = 15 000 ms. The entire sequence was repeated three times to improve signal-to-noise ratio.

Image Processing

Cortical thickness mapping. All MRIs were submitted to the CIVET pipeline (version 1.1.9). T1 images were registered to the ICBM152 nonlinear sixth-generation template with a nine-parameter linear transformation, inhomogeneity corrected (Sled *et al*, 1998) and tissue classified (Tohka *et al*, 2004; Zijdenbos *et al*, 2002). Deformable models were then used to create white and gray matter surfaces for each hemisphere separately, resulting in 4 surfaces of 40 962 vertices each (Kim *et al*, 2005; MacDonald *et al*, 2000). From these surfaces, the t-link metric was derived for determining the distance between the white and gray surfaces (Lerch and Evans, 2005). The thickness data were subsequently blurred using a 20-mm surface-based diffusion blurring kernel in preparation for statistical analyses. Unnormalized, native-space thickness values were used in all analyses owing to the poor correlation between cortical thickness and brain volume. Normalizing for global brain size when it has little pertinence to cortical thickness risks introducing noise and reducing power (Ad-Dab'bagh *et al*, 2005).

DTI Image Analysis, Whole-Brain Tractography, and Clustering Segmentation

The three repetitions were co-registered to the first $b = 0$ image in the first repetition using FSL (v. 4.0; http://www.fmrib.ox.ac.uk) to produce a new averaged image, with gradients re-oriented using a weighted least squares approach. Registration corrects eddy current distortions

and subject motion, which are important artifacts that can affect data, and averaging improves the signal-to-noise ratio. A brain mask was then generated. Points were seeded throughout each voxel of the brain. Whole-brain tractography was performed with a deterministic (streamline) approach (Runge–Kutta order two tractography with a fixed step size of 0.5 mm). More detailed descriptions of our tractography approach and our clustering segmentation algorithm can be found elsewhere (O'Donnell *et al*, 2006; Voineskos *et al*, 2009), and thus are summarized here. Threshold parameters for tractography were based on the linear anisotropy measure C_L, which provides specific advantages over thresholding using FA (Ennis and Kindlmann, 2006; Westin *et al*, 2002). The parameters chosen for this study were: $T_{seed} = 0.3$, $T_{stop} = 0.15$, and $T_{length} = 20$ (in mm). Tractography and creation of white matter fiber tracts were performed using 3D Slicer (http://www.slicer.org) and Matlab 7.0 (http://www.mathworks.com).

A pairwise fiber trajectory similarity was quantified, and the directed distances between fibers 'A' and 'B' were converted into a symmetric pairwise fiber distance. A spectral embedding of fibers was then created based on the eigenvectors of the fiber affinity matrix, and the shape similarity information for each fiber was calculated using a k-way-normalized cuts clustering algorithm (O'Donnell *et al*, 2006).

Once the whole-brain cluster model was produced, a trained operator (ANV) combined clusters corresponding to a given fiber tract. As reported elsewhere (Voineskos *et al*, 2009), excellent spatial and quantitative reliability using this clustering method (ie, both voxel overlap and scalar measures of the tensor showed high agreement) has been demonstrated. For each white matter tract, Matlab (v. 7.0) was used to calculate a mean FA (Basser and Pierpaoli, 1996) value and a mean radial diffusivity (Song *et al*, 2005) value along the selected tract. In addition, two raters with previous experience using this method, and previously determined high reliability, completed the clustering and segmentation protocols on 10% ($n = 6$) of the current sample. The intraclass correlation coefficient was measured for all tracts for both FA and radial diffusivity using a two-way mixed-effects model.

A recent fMRI investigation demonstrated that the *ZNF804A* risk variant influences connectivity between the left and right dorsolateral prefrontal cortices (Esslinger *et al*, 2009), brain regions connected by the genu of the corpus callosum (Voineskos *et al*, 2010a). This same fMRI investigation showed that this risk variant also influenced frontotemporal connectivity. Major frontotemporal white matter tracts that subserve this neuroanatomical circuitry include the cingulum bundle that connects the frontal cortex through the cingulate cortex to the hippocampal formation (Kubicki *et al*, 2003), the arcuate fasciculus, which connects Broca's area to Wernicke's area (Catani *et al*, 2005, 2007), and the uncinate fasciculus, which connects the orbitofrontal cortex to the temporal pole and the amygdala (Kubicki *et al*, 2002). Furthermore, the uncinate fasciculus and cingulum bundle have been identified as disrupted in both schizophrenia and bipolar disorder. Therefore, we segmented and measured the genu of the corpus callosum, and left and right cingulum bundle, arcuate fasciculus, and uncinate fasicuclus (Figure 1).

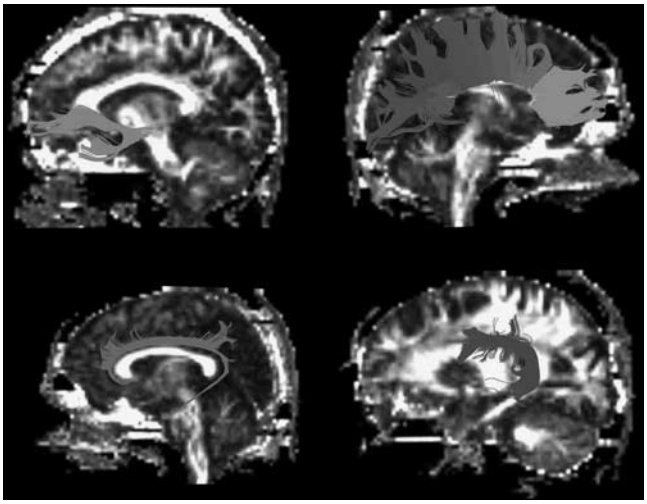

Figure 1 White matter tracts selected: clockwise from top left: uncinate fasciculus (UF), genu of corpus callosum, arcuate fasciculus (AF), cingulum bundle (CB). For each tract (left and right UF, AF, CB, and the genu of the corpus callosum), mean FA and mean radial diffusivity were calculated.

Genetics and *In Silico* Prediction

The *ZNF804A* SNPs rs1344706 (A > C) was genotyped in each subject. The SNP rs1344706 is present in the second intron of the *ZNF804A* gene (chr2:185778178, dbSNP build 131). A volume of 10 ml of venous blood was obtained from study participants, and DNA was extracted using the high-salt method (Lahiri *et al*, 1992).

Genotyping of this polymorphism was performed using a standard ABI (Applied Biosystems) 5′ nuclease Taqman assay-on-demand protocol in a total volume of 10 μl. Post-amplification products were analyzed on the ABI 7500 Sequence Detection System (ABI, Foster City, California) and genotype calls were performed manually. Results were verified independently by two laboratory personnel blinded to demographic and phenotypic information. Quality control analysis was performed on 10% of the sample.

We carried out *in silico* prediction using a 31-bp sequence including the rs1344706 C > A polymorphism to predict allele-specific binding of transcription factors (MatInspector vr. 8.0.4, Genomatix). We also explored the possibility of an experimentally verified splicing regulatory protein-binding site (SpliceAid: http://www.introni.it/splicing.html) and protein binding because of this polymorphism (Human Splicing finder: http://www.umd.be/HSF/).

Cognition

We measured effects of the *ZNF804A* variant on cognitive tests of attention control (using the Stroop Color-Word test), the cognitive domain with substantial evidence for impairment in both schizophrenia (Liu *et al*, 2002) and bipolar disorder (Quraishi and Frangou, 2002). We also measured working memory performance using the Letter Number Sequence task and verbal episodic memory performance using the List Recall task from the Repeatable Battery for the Assessment of Neuropsychological Status. Working memory and verbal episodic memory are

susceptible in both disorders, although they may be more severely affected in schizophrenia (Hill *et al*, 2008).

Statistical Analysis

Three separate analyses were performed according to the general linear model to examine the effects of the *ZNF804A* risk variant on (1) cortical thickness, (2) white matter tract integrity, and (3) cognitive performance. Two genotypic groups were created: AA homozygotes and C-allele carriers. The genotypic group served as the between-group factor in each model, and age was used as a covariate.

(1) The first model examined an ANCOVA relating the *ZNF804A* genotype to cortical thickness. Statistical thresholds were determined by application of a 5% false discovery rate (FDR) correction, where $q<0.05$ was considered significant (Genovese *et al*, 2002).

(2) The second model used a repeated-measures ANCOVA with the *ZNF804A* genotype group as the between-group factor, and age as the covariate, to examine white matter tract FA (all tract FA values were within-group measures). A similar analysis was conducted for radial diffusivity of white matter tracts.

(3) For cognitive performance, a repeated-measures ANCOVA was performed with the *ZNF804A* genotype group as the between-group factor and age as the covariate with scores on the Stroop Color-Word test, the Letter Number Sequence task, and the List Recall task as the within-group measures.

RESULTS

A 100% genotyping rate and 100% concordance rate for quality control were achieved. No difference on any demographic measures between the two genotypic groups was found (Table 1). High reliability across two raters was found for both FA and radial diffusivity measurements for all white matter tracts. For FA, the intraclass correlation coefficient (all tracts) = 0.93 ($p<0.001$), and for radial diffusivity, the intraclass correlation coefficient (all tracts) = 0.94 ($p<0.001$).

(1) A-allele homozygotes (ie, those homozygous for the risk variant) demonstrated reduced cortical thickness in the posterior cingulate gyrus ($t=4.9$, $q=0.02$), the anterior cingulate gyrus ($t=4.1$, $q=0.05$), and the superior temporal gyrus ($t=4.1$, $q=0.05$), compared with C-allele carriers (Figure 2). No other cortical regions differed significantly between genotypic groups at the 5% FDR-corrected threshold.

(2) For white matter tract FA, repeated-measures ANCOVA revealed no main effect of the genotype group ($F_{1,59}=1.2$, $p=0.3$), nor any genotype group by tract FA interaction (Greenhouse–Geiser correction: $F_{5,278}=0.4$, $p=0.9$). Similarly, no main effect of the genotype group ($F_{1,59}=0.2$, $p=0.6$) nor any group by tract interaction (Greenhouse–Geiser correction: $F_{5,287}=1.1$, $p=0.4$) was found for radial diffusivity, a measure that may be specific to myelination. We then proceeded to explore on a tract-by-tract basis whether any tracts might have been different between groups at an uncorrected $\alpha=0.05$. However, genotypic groups were not different on measures of tract FA or radial diffusivity at this significance threshold.

(3) A significant genotype group by task interaction was revealed (Greenhouse–Geisser correction: $F_{1,118}=6.0$, $p=0.01$) for cognitive performance. No main effect of the genotype was shown: $F_{1,59}=1.7$, $p=0.20$. Follow-up univariate ANCOVAs revealed a potential influence of the *ZNF804A* genotype on attention control ($F_{2,59}=4.6$, $p=0.04$), where A-allele homozygotes demonstrated reduced attention control, findings that align with those at the anterior cingulate cortex. No significant effect of genotype on working memory performance ($F_{2,59}=3.2$, $p=0.08$) or verbal episodic memory performance ($F_{2,59}=0.2$, $p=0.70$) was found (Supplementary Table S1).

In silico prediction revealed that the presence of the A allele creates a binding site for Myelin transcription factor 1-like, neuronal C2HC zinc-finger factor 1 (MYT1L, 2p25.3; matrix similarity = 0.96), whereas the presence of the C allele creates a binding site for Homeobox and leucine zipper-encoding transcription factor (HOMEZ, 14q11.2; matrix similarity = 0.92). These predictions are similar to those reported by Riley *et al* (2010). We did not identify any experimentally verified splicing regulatory protein-binding site nor any highly reliable predicted protein binding altered by this polymorphism. Furthermore, this polymorphism is present >19 kb away from the nearest exon/intron junction reducing the probability of having an important role in splicing. Therefore, the currently available evidence supports the possibility that this risk variant lies in a transcription factor-binding site, and is associated with expression of the gene.

Table 1 Participants' Characteristics

ZNF804A genotype	C-allele carriers[a] ($n=39$)	A-allele homozygotes ($n=23$)	t-test (df = 60)
	Mean ± SD	Mean ± SD	
Age (years)	37 ± 13	38 ± 12	$t=-0.3$, $p=0.74$
Education (years)	15 ± 2	16 ± 2	$t=-1.2$, $p=0.22$
Socioeconomic status[a]	49 ± 9	54 ± 7	$t=-1.8$, $p=0.07$
IQ (WTAR)	115 ± 9	119 ± 6	$t=-1.9$, $p=0.07$
Systolic BP	118 ± 12	123 ± 12	$t=-1.3$, $p=0.21$
Diastolic BP	73 ± 9	77 ± 9	$t=-1.8$, $p=0.10$
CIRS-G (ratio score)	1 ± 1	1 ± 1	$t=0.1$, $p=0.93$
	Number	Number	χ^2 (df = 1)
Gender	15 F, 24 M	7 F, 16 M	$\chi^2=0.9$, $p=0.38$

Abbreviations: BP, blood pressure; CIRS-G, Cumulative Illness Rating Scale-Geriatrics; WTAR, Wechsler Test of Adult Reading.
[a]Four factors are education, occupation, sex, and marital status.
Of the 39 C-allele carriers, 6 were homozygotes, and the sample was in Hardy–Weinberg equilibrium ($\chi^2=1.4$, $p=0.23$, df = 1).

DISCUSSION

Our main finding is that we localized effects of the *ZNF804A* risk variant to thickness of the posterior cingulate cortex, the anterior cingulate cortex, and the superior temporal gyrus, structures disrupted in both schizophrenia and

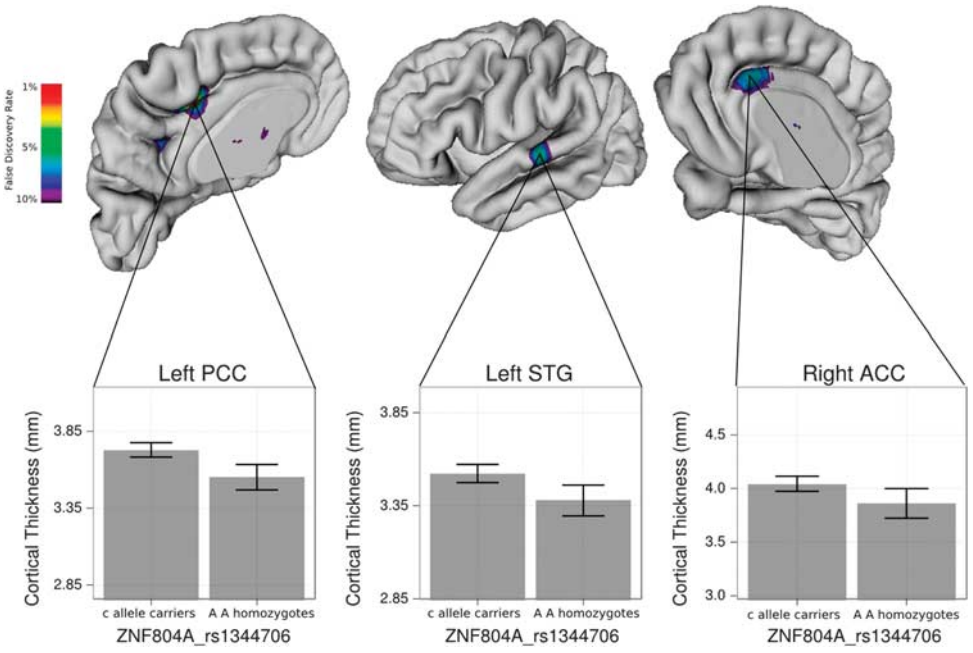

Figure 2 Influence of *ZNF804A* rs1334706 on the thickness of the posterior cingulate cortex (PCC), superior temporal gyrus (STG), and anterior cingulate cortex (ACC). Montreal Neurologic Institute space coordinates (*X*,*Y*,*Z*): PCC (−12.2, −21.6, 41.8), STG (−67.5, −19.2, 3.4), ACC (1.3, 40.6, 12.6). At each region, risk allele (AA) homozygotes demonstrated reduced thickness compared with C-allele carriers.

bipolar disorder. Furthermore, a potential association of the *ZNF804A* variant with attention control, a cognitive domain mediated primarily by the anterior cingulate cortex was found. True to the intermediate phenotype approach (Meyer-Lindenberg and Weinberger, 2006), gene effects were more penetrant at the level of the brain, rather than behavior. Taken together, our findings provide convergent evidence for the *ZNF804A* risk variant as a genetic susceptibility mechanism on at-risk neural structures and cognitive function susceptible in both schizophrenia and bipolar disorder.

The *ZNF804A* risk variant shows genome-wide significance for both schizophrenia and bipolar disorder (O'Donovan MC *et al*, 2008; Purcell *et al*, 2009) and maps onto cortical regions vulnerable in both disorders (Rimol *et al*, 2010). The influence of this variant on the right anterior cingulate cortex thickness and left superior temporal gyrus thickness is consistent with neuroimaging data implicating these regions in both disorders. The recent 'head-to-head' comparison of schizophrenia and bipolar disorder patients using cortical thickness mapping throughout the cortex found reductions in thickness of the right anterior cingulate cortex and left superior temporal gyrus in both patient groups compared with healthy controls (Rimol *et al*, 2010). These cortical thickness findings agree with earlier studies demonstrating that the superior temporal gyrus is consistently reduced in volume in schizophrenia and occasionally in bipolar disorder (Kasai *et al*, 2003; Takahashi *et al*, 2009). In parallel, the anterior cingulate cortex is characteristically affected not only in bipolar disorder but also in schizophrenia (Bora *et al*, 2010; Fornito *et al*, 2009; Szeszko *et al*, 2000). Posterior cingulate cortex volume reductions have been shown in schizophrenia and bipolar disorder patients as well (Koo *et al*, 2008; Yatham *et al*, 2007). The posterior cingulate cortex is a key node of the default network, and thus our finding that the *ZNF804A* risk variant influences thickness of this structure supports and extends another recent finding suggesting that this variant may, in part, exert risk for the major psychoses through effects on the default mode network (Lencz *et al*, 2010). Although initial evidence has accumulated for disruption of the default mode network in schizophrenia (Calhoun *et al*, 2008), recent data have suggested that bipolar disorder patients may share disruption of this network with schizophrenia patients (Ongur *et al*, 2010).

The lack of the risk variant's effect on microstructural integrity of white matter tracts was surprising, given the recent findings of impaired effective connectivity in regions connected by these tracts (Esslinger *et al*, 2009), and our *in silico* prediction of the A allele at rs1344706 as a myelin/oligodendrocyte transcription factor-binding site. Overlapping findings of white matter tract vulnerability in schizophrenia and bipolar disorder suggest that key white matter tracts (eg, the uncinate fasciculus) may serve as neural susceptibility phenotypes relevant to both disorders. White matter pathology including reductions in oligodendrocyte number and downregulation of oligodendrocyte-related genes overlap strikingly in schizophrenia and bipolar disorder, particularly in cortical regions (Tkachev *et al*, 2003). *In vivo* investigations using fMRI and cognitive performance as phenotypic probes of genome-wide significant variants are notable in that the circuitry and impaired connectivity between regions influenced by *ZNF804A* is relevant to both schizophrenia and bipolar disorder (Esslinger *et al*, 2009; Walter *et al*, 2010, March 16). For instance, in one of these investigations, altered patterns of frontotemporal and interhemispheric connectivity were demonstrated during a working memory task (Esslinger *et al*, 2009). DTI tractography offered us the opportunity to determine whether such disconnectivity and influence on

cognitive function is mediated by variation in key white matter tracts connecting these regions. Therefore, despite the considerable biological plausiblility for an effect of *ZNF804A* in white matter tracts, it is possible that *ZNF804A* exerts its effects by oligodendrocyte-related pathology in the cortical gray matter, rather than in the white matter as part of a common etiopathogenic pathway for schizophrenia and bipolar disorder.

We found that the *ZNF804A* risk variant influenced attention control, consistent with the finding of reduced thickness at the anterior cingulate cortex, the main region responsible for this cognitive function. Studies of the effects of the *ZNF804A* risk variant support its effects on cognitive domains susceptible in both schizophrenia and bipolar disorder, such as attention control (Balog *et al*, 2010) and working memory and verbal episodic memory performance (Walters *et al*, 2010), although the direction of the allelic effect across these studies is not consistent. Although we demonstrated that the *ZNF804A* variant influences superior temporal gyrus thickness, no corresponding influence on working memory was found, although there was a trend for A-allele homozygotes to perform better on the working memory task, in line with a recent investigation (Walters *et al*, 2010).

Certain limitations of our study are worth considering. The *ZNF804A* risk variant did not influence all cortical regions that may share susceptibility between schizophrenia and bipolar disorder, eg, the dorsolateral prefrontal cortex (Rimol *et al*, 2010). Although we anticipated effects of this risk variant on white matter tract integrity, it may be that other genome-wide significant variants common to the major psychoses influence white matter integrity susceptibility. It is also possible that other white matter tracts, not examined in this study, might have been influenced by this risk variant. In addition, although there is evidence to support the rs1344706 SNP as the actual risk variant within the *ZNF804A* gene (Riley *et al*, 2010; Williams *et al*, 2010), it is possible that a nearby SNP in linkage disequilibrium with rs1344706 may be the causative risk variant. Regarding cognitive performance, although a significant genotype by cognitive task interaction was found, our follow-up analysis demonstrating the effect of genotype on attention control would not have survived Bonferroni's correction. Nevertheless, this finding was valuable in that the direction of effect was the same as that for our cortical thickness findings, and, more importantly, there was biological convergence, given the risk variants' effects on the thickness of the anterior cingulate cortex. Finally, a limitation of the intermediate phenotype approach is that conclusions regarding disease severity, outcome, and treatment are difficult to make, given that disease patients (eg, those with schizophrenia and bipolar disorder) are not included for study. It is even possible that what appears to be the risk allele in healthy individuals may confer a less severe disease phenotype in patients (Donohoe *et al*, 2011; Walters *et al*, 2010). However, our work highlights the fact that the imaging-genetics intermediate phenotype strategy can be particularly useful for discovering genetically based neural risk mechanisms independent of DSM-IV- or ICD10-based diagnoses, as it is becoming increasingly clear that genetic and neural risk mechanisms cut across traditional diagnostic boundaries (Craddock and Owen, 2010).

Overlapping clinical presentations of schizophrenia and bipolar disorder have been observed since the original description of these illnesses (Craddock and Owen, 2010). A diagnosis—schizoaffective disorder—has even been created to deal with these nosological challenges. More recently, this debate has extended to neurobiological circles, as genetics and neuroimaging studies have demonstrated shared genetic vulnerability and at-risk neural circuitry, respectively, for these disorders. Our findings of a genome-wide significant variant's effects on neural structures and cognitive performance relevant to schizophrenia and bipolar disorder provide a genetic susceptibility mechanism of a shared neurobiological risk pattern for these illnesses.

ACKNOWLEDGEMENTS

This work was supported by the Canadian Institutes of Health Research Clinician Scientist Award (ANV), APA/APIRE Astra-Zeneca Young Minds in Psychiatry Award (ANV), and the Centre for Addiction and Mental Health (AT). Dr Aristotle N Voineskos had full access to all the data in the study and takes responsibility for the integrity of the data and accuracy of the data analysis.

DISCLOSURE

Dr Bruce G Pollock receives research support from the National Institute of Health and the Canadian Institutes of Health Research. Within the past 5 years, he has been a member of the advisory board of Lundbeck Canada (final meeting was in May 2009) and Forest Laboratories (final meeting was in March 2008). Dr Pollock has served one time as a consultant for Wyeth (October 2008) and Takeda (July 2007). He was also a faculty member of the Lundbeck International Neuroscience Foundation (LINF) (final meeting was in April 2010). Dr Benoit H Mulsant currently receives research support from the US National Institute of Mental Health, the Canadian Institutes for Health Research, Bristol-Myers Squibb, and Wyeth. During the past five years, he has also received research support or honoraria from Astra-Zeneca, Eli Lilly, Forest Laboratories, GlaxoSmithKline, Janssen, Lundbeck, and Pfizer. Dr James L Kennedy received speaker fees from Eli Lilly in 2010. All other authors declare no conflict of interest.

REFERENCES

Ad-Dab'bagh Y, Singh V, Robbins S, Lerch J, Lyttleton O, Fombonne E *et al* (2005). *Native Space Cortical Thickness Measurement and the Absence of Correlation to Cerebral Volume*. Paper presented at the Organization of Human Brain Mapping: Toronto.

Alexander A, Lobaugh N (2007). Insights into brain connectivity using quantitative MRI measures of white matter. In: AR McIntosh, Jirsa VK (eds). *Handbook of Brain Connectivity*. Springer: Berlin.

Balog Z, Kiss I, Keri S (2010). ZNF804A may be associated with executive control of attention. *Genes Brain Behav* **2011**: 223–227.

Basser PJ, Pierpaoli C (1996). Microstructural and physiological features of tissues elucidated by quantitative-diffusion-tensor MRI. *J Magn Reson B* **111**: 209–219.

Bora E, Fornito A, Yucel M, Pantelis C (2010). Voxel-wise meta-analysis of gray matter abnormalities in bipolar disorder. *Biol Psychiatry* **67**: 1097–1105.

Calhoun VD, Maciejewski PK, Pearlson GD, Kiehl KA (2008). Temporal lobe and 'default' hemodynamic brain modes discriminate between schizophrenia and bipolar disorder. *Hum Brain Mapp* **29**: 1265–1275.

Catani M, Allin MP, Husain M, Pugliese L, Mesulam MM, Murray RM *et al* (2007). Symmetries in human brain language pathways correlate with verbal recall. *Proc Natl Acad Sci USA* **104**: 17163–17168.

Catani M, Howard RJ, Pajevic S, Jones DK (2002). Virtual *in vivo* interactive dissection of white matter fasciculi in the human brain. *Neuroimage* **17**: 77–94.

Catani M, Jones DK, ffytche DH (2005). Perisylvian language networks of the human brain. *Ann Neurol* **57**: 8–16.

Craddock N, Owen MJ (2010). The Kraepelinian dichotomy—going, going... but still not gone. *Br J Psychiatry* **196**: 92–95.

Donohoe G, Rose E, Frodl T, Morris D, Spoletini I, Adriano F *et al* (2011). ZNF804A risk allele is associated with relatively intact gray matter volume in patients with schizophrenia. *Neuroimage* **54**: 2132–2137.

Ennis DB, Kindlmann G (2006). Orthogonal tensor invariants and the analysis of diffusion tensor magnetic resonance images. *Magn Reson Med* **55**: 136–146.

Esslinger C, Walter H, Kirsch P, Erk S, Schnell K, Arnold C *et al* (2009). Neural mechanisms of a genome-wide supported psychosis variant. *Science* **324**: 605.

First MB, Spitzer RL, Gibbon M, Williams JBW (1995). *Strucutured Clinical Interview for DSM-IV Axis I Disorders, Patient Edition (SCID-P), Version*. Biometrics Research: New York.

Fornito A, Yucel M, Dean B, Wood SJ, Pantelis C (2009). Anatomical abnormalities of the anterior cingulate cortex in schizophrenia: bridging the gap between neuroimaging and neuropathology. *Schizophr Bull* **35**: 973–993.

Genovese CR, Lazar NA, Nichols T (2002). Thresholding of statistical maps in functional neuroimaging using the false discovery rate. *Neuroimage* **15**: 870–878.

Hill SK, Harris MS, Herbener ES, Pavuluri M, Sweeney JA (2008). Neurocognitive allied phenotypes for schizophrenia and bipolar disorder. *Schizophr Bull* **34**: 743–759.

Hollingshead AB (1975). *Four Factor Index of Social Status*. Yale University: New Haven, CT.

Kasai K, Shenton ME, Salisbury DF, Hirayasu Y, Lee CU, Ciszewski AA *et al* (2003). Progressive decrease of left superior temporal gyrus gray matter volume in patients with first-episode schizophrenia. *Am J Psychiatry* **160**: 156–164.

Kim JS, Singh V, Lee JK, Lerch J, Ad-Dab'bagh Y, MacDonald D *et al* (2005). Automated 3-D extraction and evaluation of the inner and outer cortical surfaces using a Laplacian map and partial volume effect classification. *Neuroimage* **27**: 210–221.

Koo MS, Levitt JJ, Salisbury DF, Nakamura M, Shenton ME, McCarley RW (2008). A cross-sectional and longitudinal magnetic resonance imaging study of cingulate gyrus gray matter volume abnormalities in first-episode schizophrenia and first-episode affective psychosis. *Arch Gen Psychiatry* **65**: 746–760.

Kubicki M, Westin CF, Maier SE, Frumin M, Nestor PG, Salisbury DF *et al* (2002). Uncinate fasciculus findings in schizophrenia: a magnetic resonance diffusion tensor imaging study. *Am J Psychiatry* **159**: 813–820.

Kubicki M, Westin CF, Nestor PG, Wible CG, Frumin M, Maier SE *et al* (2003). Cingulate fasciculus integrity disruption in schizophrenia: a magnetic resonance diffusion tensor imaging study. *Biol Psychiatry* **54**: 1171–1180.

Lahiri DK, Bye S, Nurnberger Jr JI, Hodes ME, Crisp M (1992). A non-organic and non-enzymatic extraction method gives higher yields of genomic DNA from whole-blood samples than do nine other methods tested. *J Biochem Biophys Methods* **25**: 193–205.

Lencz T, Szeszko PR, DeRosse P, Burdick KE, Bromet EJ, Bilder RM *et al* (2010). A schizophrenia risk gene, ZNF804A, influences neuroanatomical and neurocognitive phenotypes. *Neuropsychopharmacology* **35**: 2284–2291.

Lerch JP, Evans AC (2005). Cortical thickness analysis examined through power analysis and a population simulation. *Neuroimage* **24**: 163–173.

Lichtenstein P, Yip BH, Bjork C, Pawitan Y, Cannon TD, Sullivan PF *et al* (2009). Common genetic determinants of schizophrenia and bipolar disorder in Swedish families: a population-based study. *Lancet* **373**: 234–239.

Liu SK, Chiu CH, Chang CJ, Hwang TJ, Hwu HG, Chen WJ (2002). Deficits in sustained attention in schizophrenia and affective disorders: stable versus state-dependent markers. *Am J Psychiatry* **159**: 975–982.

MacDonald D, Kabani N, Avis D, Evans AC (2000). Automated 3-D extraction of inner and outer surfaces of cerebral cortex from MRI. *Neuroimage* **12**: 340–356.

McIntosh AM, Maniega SM, Lymer GK, McKirdy J, Hall J, Sussmann JE *et al* (2008). White matter tractography in bipolar disorder and schizophrenia. *Biol Psychiatry* **64**: 1088–1092.

Meyer-Lindenberg A, Weinberger DR (2006). Intermediate phenotypes and genetic mechanisms of psychiatric disorders. *Nat Rev Neurosci* **7**: 818–827.

Narr KL, Toga AW, Szeszko P, Thompson PM, Woods RP, Robinson D *et al* (2005). Cortical thinning in cingulate and occipital cortices in first episode schizophrenia. *Biol Psychiatry* **58**: 32–40.

O'Donnell LJ, Kubicki M, Shenton ME, Dreusicke MH, Grimson WE, Westin CF (2006). A method for clustering white matter fiber tracts. *AJNR Am J Neuroradiol* **27**: 1032–1036.

O'Donovan MC, Craddock N, Norton N, Williams H, Peirce T, Moskvina V *et al* (2008). Identification of loci associated with schizophrenia by genome-wide association and follow-up. *Nat Genet* **40**: 1053–1055.

Oldfield RC (1971). The assessment and analysis of handedness: the Edinburgh inventory. *Neuropsychologia* **9**: 97–113.

Ongur D, Lundy M, Greenhouse I, Shinn AK, Menon V, Cohen BM *et al* (2010). Default mode network abnormalities in bipolar disorder and schizophrenia. *Psychiatry Res* **183**: 59–68.

Purcell SM, Wray NR, Stone JL, Visscher PM, O'Donovan MC, Sullivan PF *et al* (2009). Common polygenic variation contributes to risk of schizophrenia and bipolar disorder. *Nature* **460**: 748–752.

Quraishi S, Frangou S (2002). Neuropsychology of bipolar disorder: a review. *J Affect Disord* **72**: 209–226.

Riley B, Thiselton D, Maher BS, Bigdeli T, Wormley B, McMichael GO *et al* (2010). Replication of association between schizophrenia and ZNF804A in the Irish Case-Control Study of Schizophrenia sample. *Mol Psychiatry* **15**: 29–37.

Rimol LM, Hartberg CB, Nesvag R, Fennema-Notestine C, Hagler Jr DJ, Pung CJ *et al* (2010). Cortical thickness and subcortical volumes in schizophrenia and bipolar disorder. *Biol Psychiatry* **68**: 41–50.

Sled JG, Zijdenbos AP, Evans AC (1998). A nonparametric method for automatic correction of intensity nonuniformity in MRI data. *IEEE Trans Med Imaging* **17**: 87–97.

Song SK, Yoshino J, Le TQ, Lin SJ, Sun SW, Cross AH *et al* (2005). Demyelination increases radial diffusivity in corpus callosum of mouse brain. *Neuroimage* **26**: 132–140.

Szeszko PR, Bilder RM, Lencz T, Ashtari M, Goldman RS, Reiter G *et al* (2000). Reduced anterior cingulate gyrus volume correlates with executive dysfunction in men with first-episode schizophrenia. *Schizophr Res* **43**: 97–108.

Takahashi T, Wood SJ, Yung AR, Soulsby B, McGorry PD, Suzuki M *et al* (2009). Progressive gray matter reduction of the superior temporal gyrus during transition to psychosis. *Arch Gen Psychiatry* **66**: 366–376.

Tkachev D, Mimmack ML, Ryan MM, Wayland M, Freeman T, Jones PB *et al* (2003). Oligodendrocyte dysfunction in schizophrenia and bipolar disorder. *Lancet* **362**: 798–805.

Tohka J, Zijdenbos A, Evans A (2004). Fast and robust parameter estimation for statistical partial volume models in brain MRI. *Neuroimage* **23**: 84–97.

Voineskos AN, Farzan F, Barr MS, Lobaugh NJ, Mulsant BH, Chen R *et al* (2010a). The role of the corpus callosum in transcranial magnetic stimulation induced interhemispheric signal propagation. *Biol Psychiatry* **68**: 825–831.

Voineskos AN, Lobaugh NJ, Bouix S, Rajji TK, Miranda D, Kennedy JL *et al* (2010b). Diffusion tensor tractography findings in schizophrenia across the adult lifespan. *Brain* **133**(Part 5): 1494–1504.

Voineskos AN, O'Donnell LJ, Lobaugh NJ, Markant D, Ameis SH, Niethammer M *et al* (2009). Quantitative examination of a novel clustering method using magnetic resonance diffusion tensor tractography. *Neuroimage* **45**: 370–376.

Walter H, Schnell K, Erk S, Arnold C, Kirsch P, Esslinger C *et al* (2010). Effects of a genome-wide supported psychosis risk variant on neural activation during a theory-of-mind task. *Mol Psychiatry* **4**: 462–470.

Walters JT, Corvin A, Owen MJ, Williams H, Dragovic M, Quinn EM *et al* (2010). Psychosis susceptibility gene ZNF804A and cognitive performance in schizophrenia. *Arch Gen Psychiatry* **67**: 692–700.

Westin CF, Maier SE, Mamata H, Nabavi A, Jolesz FA, Kikinis R (2002). Processing and visualization for diffusion tensor MRI. *Med Image Anal* **6**: 93–108.

Whitford TJ, Kubicki M, Schneiderman JS, O'Donnell LJ, King R, Alvarado JL *et al* (2010). Corpus callosum abnormalities and their association with psychotic symptoms in patients with schizophrenia. *Biol Psychiatry* **68**: 70–77.

Williams HJ, Craddock N, Russo G, Hamshere ML, Moskvina V, Dwyer S *et al* (2011). Most genome-wide significant susceptibility loci for schizophrenia and bipolar disorder reported to date cross-traditional diagnostic boundaries. *Hum Mol Genet* **20**: 387–391.

Williams HJ, Norton N, Dwyer S, Moskvina V, Nikolov I, Carroll L *et al* (2010). Fine mapping of ZNF804A and genome-wide significant evidence for its involvement in schizophrenia and bipolar disorder. *Mol Psychiatry* **4**: 429–441.

Yatham LN, Lyoo IK, Liddle P, Renshaw PF, Wan D, Lam RW *et al* (2007). A magnetic resonance imaging study of mood stabilizer- and neuroleptic-naive first-episode mania. *Bipolar Disord* **9**: 693–697.

Zijdenbos AP, Forghani R, Evans AC (2002). Automatic 'pipeline' analysis of 3-D MRI data for clinical trials: application to multiple sclerosis. *IEEE Trans Med Imaging* **21**: 1280–1291.

Supplementary Information accompanies the paper on the Neuropsychopharmacology website (http://www.nature.com/npp)